

Received February 10, 2021, accepted February 12, 2021, date of publication February 16, 2021, date of current version March 1, 2021.

Digital Object Identifier 10.1109/ACCESS.2021.3059868

Biospeckle-Based Sensor for Characterization of Charcoal Rot (*Macrophomina Phaseolina* (Tassi) Goid) Disease in Soybean (*Glycine Max* (L.) Merr.) Crop

PUNEET SINGH¹, (Graduate Student Member, IEEE), AMIT CHATTERJEE¹,
LAXMAN SINGH RAJPUT², SANJEEV KUMAR², VENNAMPALLY NATARAJ²,
VIMAL BHATIA¹, (Senior Member, IEEE), AND SHASHI PRAKASH³, (Senior Member, IEEE)

¹Discipline of Electrical Engineering and Centre for Advance Electronics, Indian Institute of Technology Indore (IIT Indore), Indore 453552, India

²ICAR—Indian Institute of Soybean Research, Indore 452001, India

³Photonics Laboratory, Devi Ahilya University, Indore 452017, India

Corresponding author: Shashi Prakash (sprakash@ietdavnv.edu.in)

This work was supported in part by the Research and Development work undertaken project under the Visvesvaraya PhD Scheme of Ministry of Electronics & Information Technology, Government of India, being implemented by Digital India Corporation, Department of Science & Technology Project Grant (EMR/2016/003115/EEC), and in part by the Science and Engineering Research Board Project Grant (CRG/2018/002697).

ABSTRACT Charcoal rot is one of the most destructive fungal diseases of soybean, caused by the pathogen called *Macrophomina phaseolina*. This disease thrives in warm and dry conditions, affecting the yield of soybean and other important agronomic crops. Existing methods used to screen the disease suffer from several drawbacks including, manual rating, low accuracy, high operating time, and high system complexity. To circumvent these drawbacks, we developed a laser biospeckle based sensor to characterize the charcoal rot in soybean crop. Applicability of the proposed sensor was tested to analyze three major aspects of plant disease management, viz. characterization of disease progression, early identification of disease symptoms, and analysis of genetic resistance of the given cultivar towards the disease. The experiments were conducted during *Kharif* season for two consecutive years (2019 and 2020) on two cultivars of soybean, namely, JS 90-41 and AMS-MB-5-18. The proposed sensor as well as standard rating protocol (i.e. measuring the length of necrosis) were used to analyze the extent of disease. To characterize the disease progression and the genetic resistance of different cultivars against *M. phaseolina*, two new metrics, charcoal rot severity index and disease susceptibility index were introduced. Biospeckle activity was found to be strongly correlated with the lesion length of infected plant stems ($r = +0.96$, $p < .01$, two-tailed (for JS 90-41) and ($r = +0.95$, $p < .01$, two-tailed (for AMS-MB-5-18) for the year 2019; and $r = +0.97$, $p < .01$, two-tailed (for JS 90-41) and $r = +0.93$, $p < .01$, two-tailed (for AMS-MB-5-18) for the year 2020). Experimental results clearly indicate that the proposed sensor can be used as an efficient tool to detect the disease in its early stages of pathogen development. This study provides insights into development and implementation of disease control measures for increasing soybean crop production.

INDEX TERMS Agriculture, biospeckle activity (BA), charcoal rot, laser biospeckle, lesion length, soybean crop.

I. INTRODUCTION

Soybean (*Glycine max* (L.) Merr.) is one of the most important oilseed crops in the world, that contributes to nearly two-thirds of the world's protein and a quarter of the world's

The associate editor coordinating the review of this manuscript and approving it for publication was Derek Abbott¹.

edible oil [1]. Soybean is the primary source of protein and is extensively used to produce soy foods, cooking oil, biofuel, and regularly used for high-quality animal feed. Unfortunately, there are different kinds of diseases that can drastically affect soybean production [2], [3]. Among them, charcoal rot [4] is believed to be the most threatening and economically critical disease that hampers the soybean production

worldwide. Charcoal rot is caused by the pathogen *Macrophomina phaseolina* (Tassi) Goid [4] and can reduce the yield of multiple crop families (e.g. legume, cereal, fruit, and vegetables) up to 50%. *M. phaseolina* is a soilborne necrotrophic fungal plant pathogen that can be more severe under dry, warm, and drought conditions. The disease is so called due to gray-black discoloration resulting from the formation of microsclerotia (small black fungal survival structures) in epidermal, sub-epidermal, vascular tissues, pith regions of lower stem and root of infected plants [5].

There are three major aspects of charcoal rot management (namely, characterization of disease severity, early identification of disease symptoms, and evaluation of genetic resistance of different cultivars against the disease) that should be investigated to facilitate corrective measures for increasing crop productivity. Characterization of charcoal rot symptoms are critical due to the unavailability of appropriate fungicides that can control the disease. The most common symptoms of charcoal rot include chlorosis, plant wilting, flagging of branches, and premature senescence of plants [6]. The existing techniques used to detect the pathogen and severity of charcoal rot infection are predominantly based on visual inspection of different symptoms caused by the disease [7]. Several studies have been conducted to examine the devastating effect of charcoal rot on soybean plants in the field and laboratory conditions. The most commonly used methods to estimate infection are: Measurement of percentage chlorosis and necrosis of canopy during the growing season [8], measurement of the severity of root colonization by calculating colony forming unit (CFU) index [8], and measurements of lesion length in cut-stem inoculated plants [9]. However, these methods based on visual inspection to detect the disease are subjective and prone to error due to human perception [10]. These field screening methods to detect disease symptoms are time-consuming and labor-intensive. Several image processing software (like ASSESS 2.0) are also available to characterize the plant diseases. However, these methods use photographs of infected plant for characterizing the diseases. These methods are based on digital image processing technique comprising of the three basic steps: image processing, analysis and understanding [10]. These steps involve the pre-processing of images of plant leaf obtained from the field and perform operations including segmentation, color extraction, diseases specific data extraction and filtration of images [10]. The main limitation of image processing-based strategy is that it generally deals with the classification of diseases by analyzing color feature of infected plants or samples having visible symptoms of infection [11]. Since the visual software based disease detection methods are based on texture analysis (i.e. surface topography), both early identification of disease and evaluation of genetic resistance of different cultivars will not be possible using these techniques. Moreover, all the above discussed methods are typically applied around the physiological maturity of the plants and hence require an entire growing season which increases overall experimental tenure to a large extent.

Recently, Ahmadi *et al.* [12] reported the use of hyperspectral spectroscopy (HS) for identification of toxin effects of charcoal rot in soybean seedlings. The results of study indicated that HS can detect wilting in soybean leaves caused by pathogen. Authors, specifically concluded that the effects of disease can be prominently noticed at 1940 nm waveband. Nagasubramanian *et al.* [13] also investigated the applicability of hyperspectral imaging for identification of charcoal rot. Combination of genetic algorithm (as an optimizer) and support vector machine (as a classifier) was used for identification of maximally effective combination of wavebands that can distinguish between healthy and diseased soybean stems. However, primary disadvantage of these approaches are prohibitive cost associated with the experimental arrangements and high complexity of the processing algorithms. Fast computers, sensitive detectors, and large data storage capabilities are needed for acquiring and processing hyperspectral data. Significant data storage capability is necessary since hyperspectral cubes are large multidimensional data sets. Hyperspectral image having huge numbers of narrow and contiguous bands involves high computation complexity in processing and examining the images. Hence, dimensionality reduction becomes an essential preprocessing step for analyzing the data acquired by using hyperspectral imaging. Dimensionality reduction operation is performed by using complex algorithms (principal component analysis (PCA), singular value decomposition (SVD), multidimensional scaling (MS), pooling, and non-negative matrix factorization (NMF)) further increase the overall complexity and time required to process the data obtained from the experiments [14].

Early identification of charcoal rot symptoms is vital for sustainable management and prevention of the disease progression in host plants. Seedlings can be infected during emergence (early vegetative stages (VE)), however symptoms of the disease are not usually visible until R5 (beginning seed) to R7 (beginning maturity) growth stages [5]. Once infected, root and stem tissues are colonized within 1-3 weeks; however, there is a variation in this duration among different isolates based on the growth rate and different colony types [8]. Both, the field inspection for disease detection and small scale methods used to assess plant infection, rely on visual symptoms of the disease and fail to detect infection in early stage of pathogen developments.

Production of charcoal rot resistant cultivars is also one of the extensively practiced and reliable ways to control the plant diseases [15]. However, most of the available cultivars are not completely resistant towards charcoal rot, and only a few have been found to have certain level of resistance [5]. Identification of charcoal rot resistant cultivars from available soybean lines is challenging due to unavailability of suitable methods. Hence, it is necessary to develop consistent, reliable, and universal techniques for accurate assessment of disease-resistant capabilities in different cultivars.

As discussed in the above-mentioned sections, current methods used to detect diseases in plants have several drawbacks and cannot address every aspect of plant disease

phenotyping. Hence, development of an efficient and accurate sensor to quantify charcoal rot symptoms is essential to estimate or measure disease progression in soybean crop. Information of the quantitative parameter of disease progression is particularly important for rapid supervision and decisions, as disease management is closely related to yield loss. An effective and reliable method to detect pathogen infections in early stage of disease development is also important to reduce spread of disease and facilitate effective management practices. Moreover, there is no direct method to precisely estimate and quantify disease resistance capability of different cultivars. Therefore, development of a reliable method to analyze resistance capability of different cultivars towards *M. phaseolina* will save considerable time and is essential to screen soybean germplasm accessions at large scale with high accuracy [8].

Development and utilization of different optical techniques for precision agriculture have gained enormous popularity due to several advantages like high sensitivity, non-invasiveness, wide dynamic range, reliable operation, and capability of monitoring extensive range of chemical and biological parameters. These technologies can provide useful data that assist farmers to analyze and optimize crop production and resources. Over the past few years, different smart agricultural solutions have been developed using optics and photonics-based sensing techniques [16]–[19]. Applicability of these optical sensors as a diagnostic tool for identification and quantification of disease symptoms in different crops is challenging. In recent decades, an optical imaging technique, laser biospeckle analysis [20] has gained researchers' attention due to its different inherent advantages (e.g. fast and simple operations, low cost, non-invasive imaging). Fig. 1 shows the schematic of the basic principle associated with the generation of biospeckle phenomena. Biospeckle [21] phenomena is observed when an object having chemical or biological activity is illuminated by a coherent light source. Wavefronts of the scattered rays, reflected from the biological specimen interfere with each other and generate a granular pattern consisting of dark (for out-phase light waves) and bright (for in-phase light waves) speckle patterns, visible in the observation plane. These biological changes associated with a sample are temporal and result in intensity fluctuations in the time series biospeckle images. These intensity fluctuations are observed as a result of various physiological and biochemical processes, like microorganism interactions, cell divisions, cytoplasmic streaming, biochemical reactions, organelle movement, and Brownian motion occurring inside the samples. Over the past few years, biospeckle analysis has been extensively used in versatile applications in agriculture [21], [22], engineering [23], biomedical imaging [24], pomology [25], and biometrics [26]–[28].

In this article, we present a novel laser biospeckle based sensor for automatic detection and quantification of charcoal rot in soybean crop with high accuracy. Potential of the proposed sensor was analyzed in three different domains of plant disease management. Firstly, characterization of disease

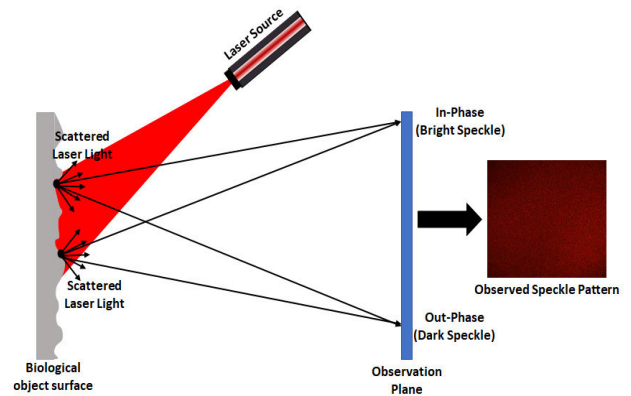


FIGURE 1. Basic principle of biospeckle generation.

progression was performed at different time intervals, and charcoal rot severity index (CSI) is proposed to analyze extent of infection in the host plants. Next, applicability of the sensor was tested to diagnose symptoms of disease in early stage of infection. Finally, disease susceptibility index (DSI) is proposed to differentiate multiple cultivars according to their disease resistance capability. The proposed indexes showed high accuracy and sensitivity in discriminating different stages of disease severity as well as analyzing resistivity of different cultivars towards the disease.

Rest of the paper is organized as follows: Section II describes materials and methods; covering sample preparation, experimental procedure, data processing algorithm, and conventional disease rating protocol. Section III presents detailed discussion of results obtained from the study. Finally, Section IV summarizes the main contributions.

II. MATERIALS AND METHODS

A. SOYBEAN SEEDLING MATERIAL AND PLANTING PROCEDURE

Two distinct soybean cultivars, namely AMS-MB-5-18 (susceptible), and JS 90-41 (moderately resistant) were selected for this study. The experiment was conducted inside a glasshouse under most favorable conditions ($30 \pm 2^\circ\text{C}$ day/ $21 \pm 2^\circ\text{C}$ night with a 12-hours photoperiod) to get the best possible symptoms expression of the disease. All the glasshouse experiments were conducted at Indian Institute of Soybean Research (IISR), Indore (India). Healthy seeds of each cultivar were selected and planted in 24-pot plastic insert. Each pot insert, having six rows of four pots, was filled with soil and sand, and recommended dose of fertilizer was used [8]. Two weeks after the emergence (V2 growth stage), plants were thinned down and only one most vigorous plant per pot was allowed to grow.

B. PREPARATION AND CUT-STEM INOCULATION OF PATHOGEN

To prepare the fungal toxin, *M. phaseolina* was isolated from heavily infected stem samples collected from an experimental field of the plant pathology, Jawaharlal Nehru Krishi

Vishwavidyalaya (JNKVV), Jabalpur (India). The infected stem was washed thoroughly with distilled water and dried for 1 hour. Washed infected stem was surface sterilized with 0.1% solution of NaCl for one minute. After surface sterilization stem samples were cut down into small pieces (nearly 0.5 cm) with the help of sterilized blade and washed thrice in sterilized distilled water. Then small pieces of stem was dried on sterilized blotter paper and inoculated on potato dextrose agar media (HiMedia, India) in a laminar air flow chamber and finally incubated at 27 °C in the BOD chamber [29], [30]. The production of sclerotia and morphology of the fungus colony were the main criteria used to identify the *M. phaseolina* [31]. Moreover, *M. phaseolina* was also identified with its microscopic characteristics such as right angle branch of hyphae with constriction at origin point and production of sclerotia [30]. The images of typical fungi culture and its microscopic structure are shown in Fig. 2 (a) and (b) respectively. Finally, four days old culture was used for inoculation on soybean plants.

We conducted the experiments during *Kharif* season of two consecutive years 2019 and 2020 to characterize the effect of charcoal rot with twenty replication of each sample by using the cut stem inoculation technique [9]. Completely randomized block design was used for the experiments. 400 uniformly grown plants were selected and randomly separated into two groups; namely, healthy and diseased for each cultivar. No inoculation was performed for the plants of healthy group, whereas for diseased group *M. phaseolina* was inoculated on plant stem.

For inoculation, stem apex of each plant was severed 25 mm above the unifoliate node after 15 days of planting by using a sharp razor blade. Sterile 200 μ l pipette tip (Fisher Scientific) was used to inoculate pathogen on plant stems. Open end of pipette was inserted down into actively growing *M. phaseolina* culture, and small circular disk of fungal mycelium with agar was removed from the culture plate. Pipette tip containing actively growing pathogen was instantly used for the inoculation. Pipettes were directly placed on the cut stems and pushed down as far as possible in order to embed the fungal mycelia into the wounded cut stem apex.

C. HARDWARE SETUP AND DATA ACQUISITION PROCESS

Hardware setup used for the experiment is shown in Fig. 3. He-Ne diode laser (15 mW, $\lambda = 632.8$ nm) was utilized to illuminate the treated plant stem. The intensity of the laser beam was controlled by using variable attenuator. Spatial filtering arrangement, consisting of microscopic objective (MO) of total magnification 40X and an aperture of 10 micrometer, was used to filter and expand the beam. Filtering arrangement reduces the non-uniformity generated due to noise in the laser profile to a considerable extent and produces a uniformly illuminated laser beam. The biospeckle imaging of the healthy and diseased plants was performed destructively at different time points after inoculation. All leaves were removed from plant stem and

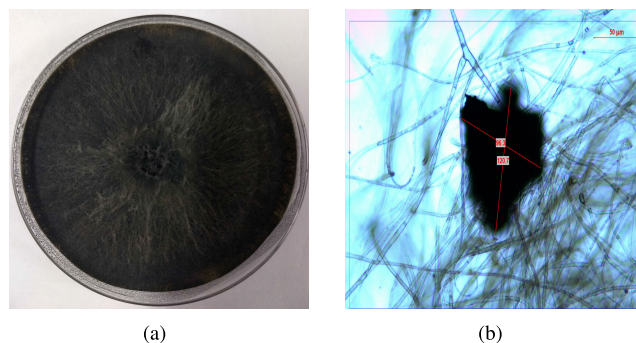


FIGURE 2. (a) Culture of *M. phaseolina* isolated from charcoal rot of soybean stem on PDA plate at 4 days after incubation, and (b) mycelium and sclerotia of *M. phaseolina* under light microscope at 20 \times .

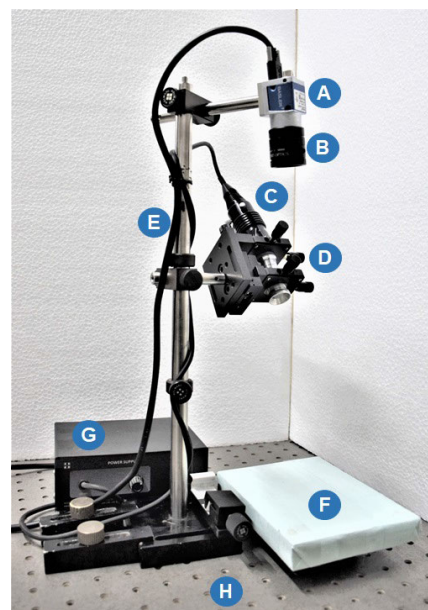


FIGURE 3. Experimental setup used for biospeckle analysis: CCD camera, lens assembly, laser source, spatial filtering arrangement, mount, sample space, laser power supply and vibration isolation table top.

the stem was detached from the soil surface immediately prior to biospeckle analysis. Stems were placed on a vibration isolation table top, and illuminated with filtered and expanded laser beam for biospeckle imaging. Plant stems were imaged at different time intervals after inoculation. Successive biospeckle images corresponding to each sample were recorded by a CCD camera (Basler Corp., frame rate: 30 fps, resolution: 1024 \times 967). To study the biospeckle behavior of plant stems in early stages and at later time instants, biospeckle images of both the groups were recorded every day after inoculation (DAI) of pathogen. Data collection associated with the disease progression was completed within 10 DAI. Stack of time frame sequence of these encoded images were created and processed in MATLAB.

D. DATA PROCESSING

In order to extract biological activity present in a healthy and diseased stem cells, n-speckle frames of size M \times N are

captured at a sampling rate of $f = n/t$, where t is the time duration for recording all the speckle frames. Activity associated with the healthy and the diseased group was calculated by considering only active data points from the speckle images. The overall processing strategy used to analyze BA of the samples is given below:

- 1) Time series of speckle patterns of both groups (healthy and diseased) for different time intervals are recorded and a stack is created using MATLAB for further processing.
- 2) An image mask is generated to automatically select region of interest (ROI) from the speckle images captured for both the groups. To generate ROI mask, image segmentation is performed [32]. The purpose of image segmentation is to partition an image into number of segments. Each segment contains some pixels that belong to one of the specific groups; and the number of groups are often predetermined in practice. Simplest strategy for image segmentation is thresholding, as it usually needs information embedded in the pixel levels of an image. In this work, we have utilized the strategy based on Otsu's binarization [32] for automatic selection of ROI from speckle images. This method calculates the optimum binarization threshold using a probabilistic approach. Algorithm returns a single intensity threshold that can separate image pixels into two classes, namely foreground and background. To generate a mask, single image from particular image stack is chosen and binarized using Otsu's thresholding. In this method, an image is partitioned into two classes C_1 and C_2 having gray levels $[0 - L]$ such that $C_1 = \{0, 1, 2, \dots, T\}$ and $C_2 = \{T + 1, T + 2, T + 3, \dots, L - 1\}$ by using threshold at level T . Value of threshold T is determined by minimizing within-class variance, equivalently maximizing the between-class variance to separate foreground and background. To calculate optimum threshold, mean of two classes is calculated as:

$$\mu_{C_1} = \sum_{n=0}^T \frac{np_n}{P_{C_1}} \quad (1)$$

$$\mu_{C_2} = \sum_{n=0}^T \frac{np_n}{P_{C_2}} \quad (2)$$

where p_n is defined as the probability of occurrence of the n^{th} gray level. P_{C_1} and P_{C_2} are the probabilities associated with the occurrence of two classes.

Finally associated variance for both the classes (C_1 and C_2) is described as [27]:

$$\sigma^2(T) = P_{C_2} \times P_{C_2} ((\mu_{C_1} - \mu_{C_2}))^2 \quad (3)$$

From the above equations, optimum threshold T^* for given image can be computed as:

$$T^* = \arg \max_{0 < T < L-1} \sigma^2(T) \quad (4)$$

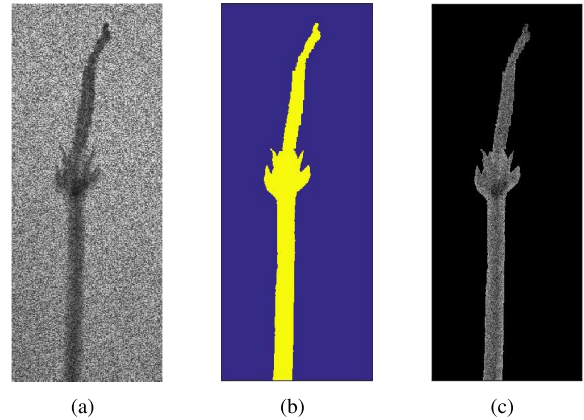


FIGURE 4. (a) Speckle image for soybean stem, (b) generated image mask, and (c) masked speckle image.

This threshold value (T^*) is used to generate an image mask with zero gray level for background and one for active data points. Finally, only active pixels corresponding to object under study is selected from speckle image by multiplying each speckle frame with the generated mask. Speckle image of a plant stem is shown in Fig. 4 (a), and its corresponding image mask is given in Fig 4 (b). Resultant masked overlaid image for given speckle frame is shown in Fig. 4 (c).

- 3) Masked images generated by using Otsu's binarization in step (ii) were used for biospeckle analysis. Once the ROI is selected, BA associated with different groups is analyzed using a methodology based on random time history of speckle pattern (RTHSP) followed by co-occurrence matrix (COM) [33]. Activity recorded in multiple speckle frames is encoded into a single matrix by generating its RTHSP. This method can quantify the BA with higher accuracy by considering the optical inhomogeneity present in the samples. Moreover, as the inhomogeneity present in BA map increases, the efficiency of the proposed method also increases [33]. To generate RTHSP, multiple random points (say R) are selected from the recorded speckle pattern and placed next to each other. The locations of these points are fixed for all the successive time frame images. When a sample presents low biospeckle activity, time variation of successive speckle patterns is slow and results in elongated shape of the RTHSP. However, phenomena showing high biospeckle activity possesses greater change in successive speckle sequences, and generate RTHSP which resembles an ordinary speckle pattern.
- 4) After generation of RTHSP, COM [34] is created by calculating number of successive occurrences of every pixel pair in each row of the RTHSP, and is given by:

$$M_{COM} = [N_{i,j}] \quad (5)$$

where, N is the occurrence of certain pixel value index i , instantly followed by pixel value index j . For low BA, pixel values of COM does not change much, and

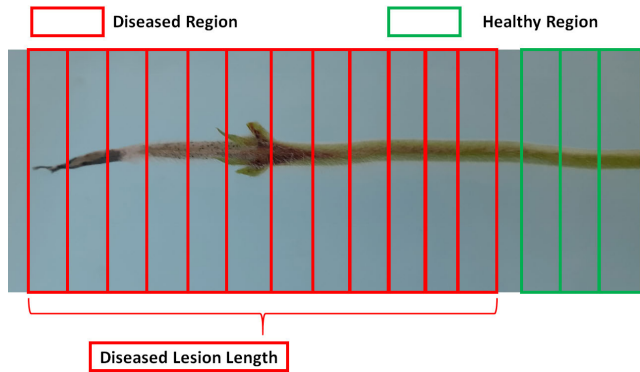


FIGURE 5. Healthy and diseased region present in soybean plant stem after inoculation.

most of non-zero pixel values are confined towards the principal diagonal. Resultant matrix is sparse in nature and most of its elements are zero. In case of high BA, COM resembles a cloud like pattern around the principal diagonal. In the next step, normalization of the COM is performed as given below:

$$M_{i,j} = \frac{N_{i,j}}{\sum_{i,j}(N_{i,j})} \quad (6)$$

- 5) Finally, numerical quantification of BA is performed by calculating the spread of normalized COM values around the principal diagonal by using first order moment called absolute value of difference (AVD) [33]. The method calculates sum of the difference between normalized COM values, multiplied by its distance from the principal diagonal, and is given by:

$$AVD = \sum_{i,j} M_{i,j} |i - j| \quad (7)$$

E. CHARCOAL ROT RATING PROTOCOL

In addition to biospeckle analysis, disease progression was manually rated by measuring linear necrosis or lesion length (in centimetre) caused by *M. phaseolina*. The pipette tips were removed from each plant stem just three DAI and discarded to measure necrosis produced by the pathogen. Severity of the disease was measured by a ruler/scale and recorded every day until end of the experiment. Fig. 5 shows the different regions (healthy and diseased) present in the plant stem.

F. STATISTICAL ANALYSIS

The obtained data was statistically analyzed by using IBM SPSS statistics software (version 16.0). Twenty measurements from each seedling were averaged for an experimental unit. ANOVA was used to compare the mean values of the data acquired for both the groups (healthy and diseased) and to find the statistical significance ($p \leq 0.05$) between these mean values [34]. The main hypothesis for this analysis was to analyze the possible effect of pathogen infection on

biospeckle activity recorded at different time intervals for two cultivars (AMS-MB-5-18 and JS 90-41). We analyzed the measurement events separately by considering the biospeckle activity as a dependent variable and the time duration of the treatments and cultivars as an independent variable. ANOVA was used for testing cultivars \times time interaction and its effect on biospeckle activity. Differences among the means for all the measurement events were tested for significance by using Tukey's honest significant difference test (Tukey's HSD). Additionally, relationship between BA and lesion length was analyzed using Pearson's correlation coefficients (R).

III. RESULTS AND DISCUSSION

A. CHARACTERIZATION OF DISEASE PROGRESSION

Cultivars with susceptible and moderately resistant response towards charcoal rot were used for this study. Measurements were carried out for two consecutive years (2019 and 2020 in *Kharif season*) on both the cultivars (AMS-MB-5-18 and JS 90-41), containing healthy and diseased groups. Visual images of both the soybean cultivars, infected with *M. phaseolina* for different time intervals are presented in Fig. 6 and 7. Biospeckle data corresponding to different time intervals for each group was also recorded for different time duration and analyzed using the strategy discussed in Section II. Fig. 8 (a) and (b) show RTHSP corresponding to healthy group for JS 90-41 cultivar. Resultant COM generated from the biospeckle data are shown in Fig. 8 (c) and (d) respectively. Elements of COM for healthy plants do not show much variations and are confined around the principal diagonal for all the time duration. BA results corresponding to diseased group are shown in Fig. 9. For diseased plants, on the 0th day, the shape of COM was observed to be similar as healthy group. However, as the exposure time of the pathogen increases, higher BA was observed, and resultant COM creates a distributed cloud of high values around the principal diagonal.

BA for all the acquired data was calculated by using AVD method and plotted against time. BA of JS 90-41 and AMS-MB-5-18 cultivars corresponding to different time intervals for the year of 2019 and 2020 are shown in Fig. 10 (a) and (b) respectively. BA of both the cultivars for healthy plants at all the measurement stages was almost constant. However, distinct change in BA of diseased group as compared to healthy one was observed. For the diseased group, BA increased continuously with time for both the cultivars as shown in Fig. 10. This change in BA of diseased group was observed due to toxin and enzymatic effects of the pathogen that degrade [5] stem tissues as time progresses. This degradation occurred due to the infection which colonized within a few days and ultimately resulted in death of the plants. In the diseased group, pathogen enhances the rate of respiration, and activity of enzymes associated with the respiration process, which in turn increases the metabolism of infected region [35]. Moreover, biospeckle activity is also strongly affected by several phenomena related to different vital metabolic processes namely reserve mobilization,

TABLE 1. Biospeckle activity and lesion length associated with healthy and diseased groups for *Kharif* season of year 2019.

Cultivars	JS 90-41			AMS-MB-5-18		
	Healthy	Diseased		Healthy	Diseased	
	Biospeckle Activity	Biospeckle Activity	Lesion Length	Biospeckle Activity	Biospeckle Activity	Lesion Length
0	1.16×10^{3a}	1.17×10^{3a}	0 ^a	1.17×10^{3a}	1.19×10^{3a}	0 ^a
1	1.15×10^{3a}	1.31×10^{3b}	0 ^a	1.12×10^{3a}	1.32×10^{3ab}	0 ^a
2	1.17×10^{3a}	1.39×10^{3c}	0 ^a	1.16×10^{3a}	1.50×10^{3c}	0 ^a
3	1.09×10^{3a}	1.72×10^{3d}	0.21 ^{ab}	1.10×10^{3a}	2.01×10^{3d}	0.46 ^{ab}
4	1.12×10^{3a}	1.83×10^{3de}	1.37 ^b	1.15×10^{3a}	2.22×10^{3cde}	2.76 ^b
5	1.16×10^{3a}	1.91×10^{3def}	1.64 ^{cd}	1.09×10^{3a}	2.40×10^{3ef}	3.87 ^{bd}
6	1.07×10^{3a}	2.39×10^{3g}	1.83 ^{de}	1.11×10^{3a}	2.73×10^{3fg}	4.73 ^{de}
7	1.04×10^{3a}	2.50×10^{3gh}	2.06 ^{def}	1.08×10^{3a}	3.47×10^{3gh}	5.28 ^{df}
8	1.13×10^{3a}	2.82×10^{3h}	3.24 ^f	1.12×10^{3a}	4.03×10^{3h}	5.79 ^{dg}
9	1.04×10^{3a}	3.45×10^{3i}	3.87 ^g	1.08×10^{3a}	4.40×10^{3i}	6.87 ^h

Values are rounded off to the nearest integer up to two place of decimal for the given numerical data. The values superscripted with different letter in same column are significantly different at $p \leq 0.05$ (Tukey's Honest Significant Difference test).

TABLE 2. Biospeckle activity and lesion length associated with healthy and diseased groups for *Kharif* season of year 2020.

Cultivars	JS 90-41			AMS-MB-5-18		
	Healthy	Diseased		Healthy	Diseased	
	Biospeckle Activity	Biospeckle Activity	Lesion Length	Biospeckle Activity	Biospeckle Activity	Lesion Length
0	1.13×10^{3a}	1.29×10^{3a}	0 ^a	1.13×10^{3a}	1.37×10^{3a}	0 ^a
1	1.04×10^{3a}	1.47×10^{3ab}	0 ^a	1.12×10^{3a}	1.71×10^{3b}	0 ^a
2	1.18×10^{3a}	1.64×10^{3c}	0 ^a	1.21×10^{3a}	2.10×10^{3c}	0 ^a
3	1.14×10^{3a}	1.83×10^{3cd}	0.23 ^{ab}	1.03×10^{3a}	2.18×10^{3d}	0.52 ^{ab}
4	1.16×10^{3a}	1.90×10^{3c}	1.41 ^{bc}	1.13×10^{3a}	2.35×10^{3de}	3.24 ^{bc}
5	1.14×10^{3a}	2.09×10^{3ef}	1.59 ^{cd}	1.28×10^{3a}	2.65×10^{3e}	4.14 ^d
6	1.17×10^{3a}	2.40×10^{3def}	1.78 ^{de}	1.29×10^{3a}	2.95×10^{3ef}	4.92 ^{de}
7	1.12×10^{3a}	2.65×10^{3g}	2.15 ^f	1.13×10^{3a}	3.53×10^{3g}	5.263 ^{df}
8	1.10×10^{3a}	2.95×10^{3h}	3.54 ^{fg}	1.04×10^{3a}	4.26×10^{3h}	6.14 ^{gh}
9	1.11×10^{3a}	3.57×10^{3i}	4.01 ^h	1.08×10^{3a}	4.72×10^{3i}	7.21 ^h

Values are rounded off to the nearest integer up to two place of decimal for the given numerical data. The values superscripted with different letter in same column are significantly different at $p \leq 0.05$ (Tukey's Honest Significant Difference test).

glyoxylate cycle, phytohormonal regulation, and respiration process in biological tissues [36]. These physiological changes result in variation in the biospeckle index of the recorded biospeckle data.

Descriptive statistics of BA associated with both the cultivars (healthy and diseased groups) for 2019 *Kharif* season is given in Table 1. Similarly, all the data acquired in the year 2020 is provided in Table 2. For healthy group, no significant difference ($p < 0.05$) was observed among the biospeckle readings taken at different time intervals for both the years. ANOVA for biospeckle measurement corresponding to disease group indicated no significant difference ($p < 0.05$) for $t = 0^{\text{th}}$ day and its biospeckle behavior was similar to healthy group. However, progression of disease symptoms can be clearly traced by BA for diseased group. There was a significant difference ($p < 0.05$) in BA related to the diseased group for different time intervals during both the years. BA corresponding to diseased plants increased

continuously with time as duration of the pathogen interaction increased.

Ability of the proposed sensor to identify disease symptoms with high accuracy was tested and compared with commonly used method based on lesion length measurement. Disease progression was manually rated by calculating lesion length in every stage of plant growth. Table 1 and 2 show lesion length (in cm) associated with both the cultivars obtained in the years 2019 and 2020 respectively. Visible appearance of healthy plants was similar at all the measurement stages. However, the diseased plants had signs of increased lesion length, which was visible after few DAI (Fig. 6 and 7). Identification of disease length progression is very important for analyzing severity of disease and resistivity of different cultivars towards pathogen. This is the most commonly used method for manual rating of disease symptoms. Lesion length measurements corresponding to diseased group were undertaken just 3 DAI at different time intervals

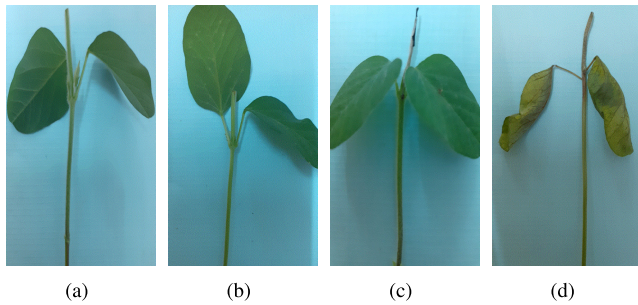


FIGURE 6. Visual images for diseased group of JS 90-41 cultivar at (a) $t = 0^{\text{th}}$ day, (b) $t = 2^{\text{nd}}$ day, (c) $t = 5^{\text{th}}$ day, and (d) $t = 9^{\text{th}}$ day.

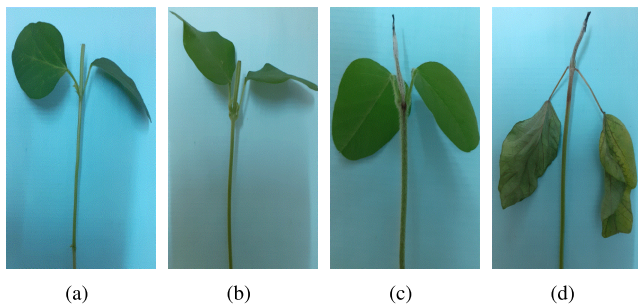


FIGURE 7. Visual images for diseased group of AMS-MB-5-18 cultivar at (a) $t = 0^{\text{th}}$ day, (b) $t = 2^{\text{nd}}$ day, (c) $t = 5^{\text{th}}$ day, and (d) $t = 9^{\text{th}}$ day.

and compared with the corresponding BA. Correlation of BA with lesion length of diseased group at every stage of disease progression was performed. BA presented significant high positive correlation ($r = +0.96$, $p < .01$, two-tailed (for JS 90-41 cultivar) and $r = +0.95$, $p < .01$, two-tailed (for AMS-MB-5-18 cultivar) for year 2019 and $r = +0.97$, $p < .01$, two-tailed (for JS 90-41 cultivar) and $r = +0.93$, $p < .01$, two-tailed (for AMS-MB-5-18 cultivar) for year 2020) with lesion length. Obtained data indicate that the proposed sensor can be used as an alternative non-destructive method to detect symptoms of charcoal rot in soybean.

To quantify the progression of disease symptoms and to evaluate severity of the pathogen infection automatically by using BA of diseased group, CSI is introduced. This index is given as the ratio of the mean difference of BA associated with diseased and healthy groups for a given day, to the average of BA associated with healthy group for all the measurement events. It is mathematically expressed as:

$$(CSI)_i = \frac{d_i - h_i}{\sum_{i=0}^{D-1} (h_i)/D} \quad (8)$$

where, D is the number of days of observation, d_i and h_i are the BA corresponding to different time intervals for diseased and healthy groups respectively.

Fig. 11 (a) and (b) show the disease progression for CSI corresponding to diseased group at different time intervals during the years 2019 and 2020, respectively. CSI is a measure of disease progression and hence can provide information related to different stages of disease severity. The value of

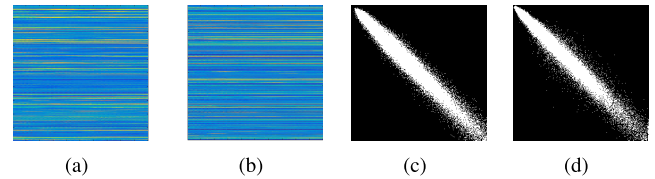


FIGURE 8. RTHSP for healthy group of JS 90-41 cultivar (a) $t = 0^{\text{th}}$ day, (b) $t = 9^{\text{th}}$ day; COM for healthy group (c) $t = 0^{\text{th}}$ day, (d) $t = 9^{\text{th}}$ day.

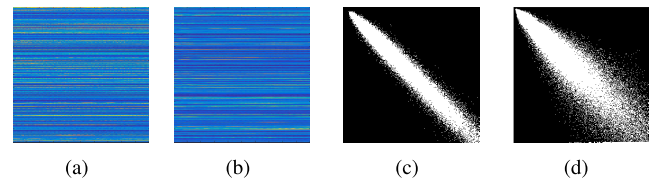
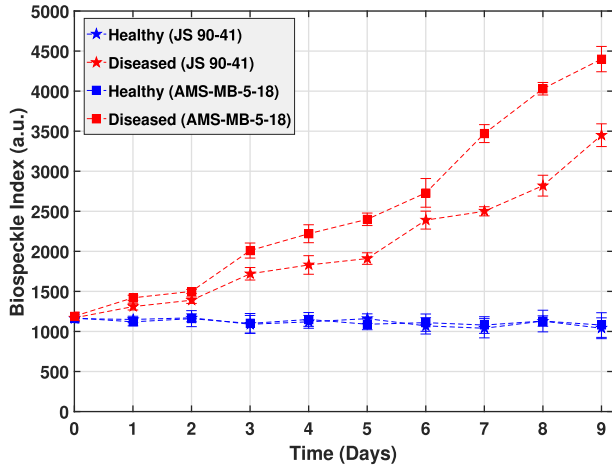


FIGURE 9. RTHSP for diseased group of JS 90-41 cultivar (a) $t = 0^{\text{th}}$ day, (b) $t = 9^{\text{th}}$ day; COM for diseased (c) $t = 0^{\text{th}}$ day, (d) $t = 9^{\text{th}}$ day.

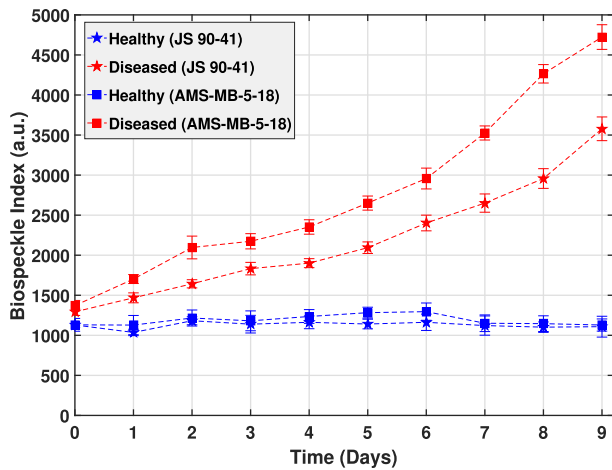
this ratio close to zero indicated no infection. The higher the ratio, the greater the severity of disease on soybean plants. Continuous increase in CSI values was observed for both the cultivars as time of the pathogen interaction with plants increased as shown in Fig. 11 (a) and (b). Similar to the diseased plants lesion length, CSI also presented the highest change for the 9th day measurement. CSI presented high positive correlation with lesion length ($r = +0.96$, $p < .01$, two-tailed (for JS 90-41) and $r = +0.95$, $p < .01$, two-tailed (for AMS-MB-5-18)) for the year 2019 and ($r = +0.97$, $p < .01$, two-tailed (for JS 90-41) and $r = +0.91$, $p < .01$, two-tailed (for AMS-MB-5-18)) for the year 2020, which show that the sensor can accurately analyze progression of the disease in plants. Hence, we propose this ratio for relative comparison of different stages of disease progression. CSI showed a promising performance to analyse the extent of charcoal rot severity in diseased plants and can be used in different studies as a new metric to improve the disease detection capability.

B. EARLY IDENTIFICATION OF CHARCOAL ROT SYMPTOMS

Ability of a sensor to detect pathogen in early stages is very important for mitigation of disease by incorporating corrective measures. *M. phaseolina* can infect soybean at all growth stages. Infection at early stages can result in seedling death or the disease can progress in the form of latent infection and aggravates during maturity when plant starts senescing. Therefore, early detection of latent infection for timely control measures is of economic significance [38] in soybean crop. Data obtained from the proposed sensor clearly indicates that the BA for both the cultivars are responsive towards the disease symptoms even at early stages of infection. Non-inoculated plants remained healthy for entire experimental duration and presented almost constant BA (Table 1 and 2). Plant stems inoculated with *M. phaseolina* were initially colonized without symptoms. These symptoms became visible on the stem cells after a certain latency period, before that plant appeared to be healthy [39]. As shown in



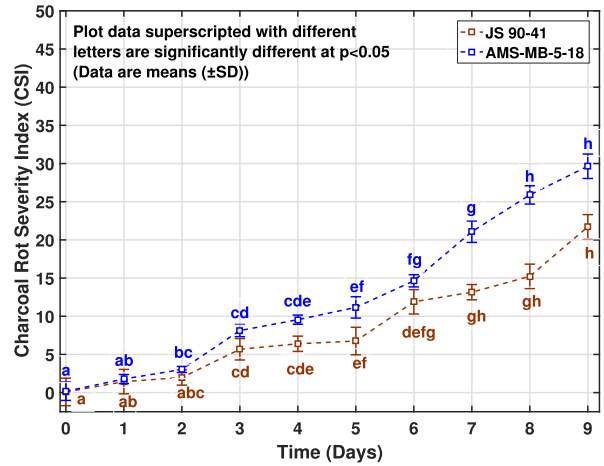
(a)



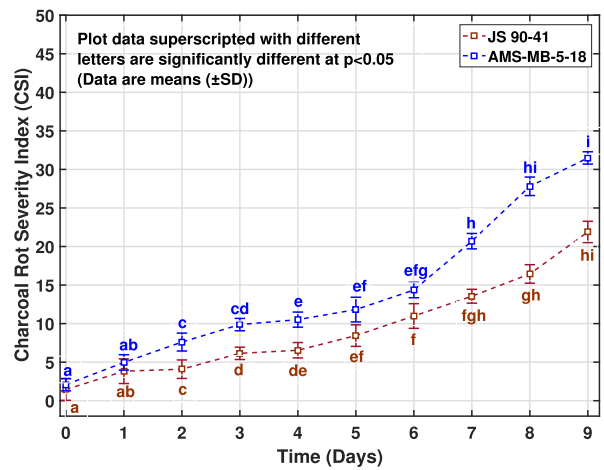
(b)

FIGURE 10. BA of JS 90-41 and AMS-MB-5-18 associated with healthy and diseased plant stems at different time intervals for (a) year 2019, and (b) year 2020.

Fig. 10 (a) and (b), progression of the disease in early stages of plant can be clearly distinguished by analysing BA of the samples acquired using the sensor, which was not observable by manual inspection. Initially, just after the inoculation, BA of healthy and diseased plants was similar, and there was no significant difference ($p < 0.05$) in the acquired data. However, just two DAI, BA of diseased group increased significantly, whereas change in BA of healthy group was insignificant ($p < 0.05$). Moreover, during this stage lesion length of charcoal necrosis produced due to disease was not even observable. Usually, charcoal necrosis is visible in four to five DAI; before that we cannot measure disease severity by using routine manual methods. As shown in Fig. 10 (a) and (b), BA of diseased group increased prominently just two DAI. This increase in the BA index is occurred due to metabolic changes associated with the progression of disease through stem cells. Moreover, CSI also increased significantly ($p < 0.05$) for both the cultivars just two DAI



(a)



(b)

FIGURE 11. Charcoal rot severity index (CSI) associated with both the cultivars at different time intervals for (a) year 2019, and (b) year 2020.

which imply that by using the proposed method the disease symptoms can be identified even in early stage of infection (Fig. 11).

C. ANALYSIS OF DIFFERENCES IN GENETIC RESISTANCE AGAINST THE DISEASE

Generation of charcoal rot resistant cultivars is one of the most common and reliable ways to manage the disease in soybean crop. Development of an automatic and accurate sensor to characterize the resistivity of different cultivar towards *M. phaseolina* is an important and much needed step for plant breeding programs. One of the objectives of this investigation is to analyze the capability of developed sensor to identify resistivity of different cultivars towards the disease. To investigate this, two distinct cultivars of soybean with known differences in disease resistance were used. We have tested applicability of the proposed sensor to categorize soybean cultivars in terms of their capability to resist the disease in a given environmental conditions. There is no direct method

that can precisely quantify the susceptibility of the soybean cultivars towards charcoal rot, hence a new metric called DSI was introduced. This is mathematically expressed as:

$$(DSI)_i = \frac{\sum_{i=0}^{D-1} (d_i - h_i)}{D} \quad (9)$$

As shown in Fig. 11, severity of the disease was also higher for susceptible cultivar at every time point of disease progression. To compare the ability of DSI to identify susceptible and resistant soybean cultivars towards the disease, conventional method based on the calculation of area under the disease progress curve (AUDPC) was also utilized [40]. AUDPC provides useful quantitative measure of disease intensity over time. AUDPC for the given disease progress curve (Fig. 11) is calculated as:

$$AUDPC = \sum_{i=0}^{D-1} \frac{y_i + y_{i+1}}{2} \times (t_i - t_{i+1}) \quad (10)$$

where y_i is intensity of disease at the i^{th} day of observation, t_i is time (in days) at the i^{th} observation, and D is the total number of days of observations.

To analyze level of resistance of both the cultivars (JS 90-41 and AMS-MB-5-18) against *M. phaseolina*, a comparison of obtained DSI and AUDPC was performed. The higher the value of DSI and AUDPC, the lower the resistivity of the given cultivar. Comparison of DSI and AUDPC values was performed for both the cultivars by using the data acquired in both the years 2019 and 2020, and is given in Fig 12 (a) and (b) respectively. Significantly higher values of DSI (1308.25 and 1634.47) was obtained for AMS-MB-5-18 as compared to JS 90-41 (936.73 and 1053.57). AUDPC calculated for the disease curve also showed higher values (110.17 and 124.43) for AMS-MB-5-18 as compared to JS 90-41 (73.43 and 81.69) cultivar. This suggests that the resistivity of AMS-MB-5-18 is lower as compared to the JS 90-41 cultivars. The values of charcoal necrosis length (given in Table 1 and 2) also presented similar behavior. For AMS-MB-5-18, lesion length is increased at higher rate as compared to JS 90-41 and pathogen colonized early in AMS-MB-5-18 cultivar. The responses of resistant cultivars towards virus infection are generally characterized by marked metabolic changes associated with the occurrence of defense reactions. These reactions are related to the secretion of several enzymes which inhibits the development of pathogens inside the plants [35] and results in decrease in BA associated with the given plant sample.

Moreover, visual perception based method require intrinsic skills and more time to trace the symptoms of disease as well as speed of infection development to analyze the resistivity of different cultivars towards the disease. It is evident from the visual images shown in Fig. 6 and 7 that perception based analysis require at least five to seven DAI to analyze the susceptibility of given cultivars towards charcoal rot. On the other hand, by analyzing the BA of diseased groups charcoal rot susceptibility of the cultivars can be traced by only two

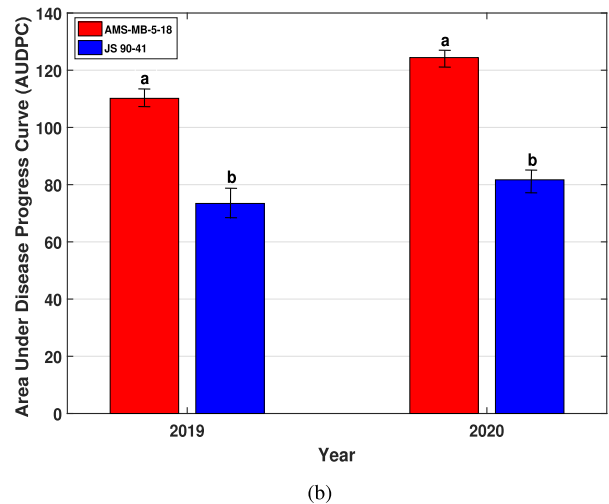
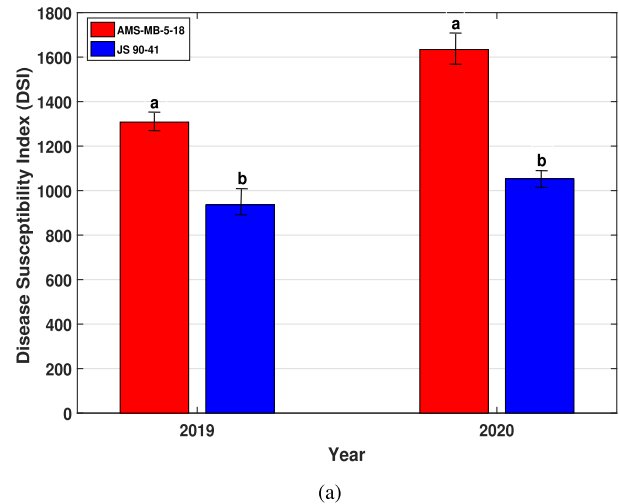


FIGURE 12. Comparison of (a) disease susceptibility index (DSI), and (b) area under disease progress curve (AUDPC) associated with both the cultivars for different years.

to three DAI, since BA for susceptible cultivar increases rapidly as compared to the resistant one. Data acquired from the experiments indicated that the sensor provides accurate and rapid identification of disease resistance capability of given cultivars. It is also evident from the results that newly developed index can be used for precise determination of disease resistance ability of different cultivars and can be used as a performance metric for automatic identification of cultivars resistant towards a disease.

As discussed, the advantages of the proposed sensor as compared with the existing strategies include its extreme simplicity, minimal-cost, high-operating speed, non-invasive identification, user-friendliness, and high performance efficiency. In this experiment, low-cost components (diode laser, beam expander, and CCD camera) are utilized for biospeckle analysis setup. Hence, the overall system cost is approximately USD 1500. Moreover, due to enormous advancement in imaging and fabrication technology, cost-effective biospeckle sensors have also been developed using android

phone or webcam in the recent years [25], [39]. This can further reduce the system cost by using off the self-commodity hardware costing about USD 100. Moreover, measurement of speed of the sensor includes its data acquisition speed and data processing speed. Speed of operation to assess the overall dynamicity associated with the biospeckle data depends upon the type of data processing technique. Numerical indexing and visual analysis based method have been widely utilized in the literature for analyzing the biospeckle data, [40]. In this work, overall acquisition time is 3.4 seconds (as photographs are captured with a camera of frame rate = 30fps), and processing time (t_p) is approximately 4.2 seconds (for RTHSP based numerical method). However, for full-field analysis based visual methods possess relatively high processing time as compared to the method used in the present study. The value of t_p was observed to be 15.8 seconds for single summation based Fujii's method [40], and 305.46 seconds for double summation based generalized difference (GD) [39] method. For calculating the code execution time, 'tic toc' profiler in MATLAB 2016a (core i5, 5th generation, 16 GB RAM, 64 bit OS, Windows 10 configuration) was used. Further investigations are underway to develop a compact assembly by using time-synchronized low-cost USB camera (with a miniaturized auto-focusing lens) to produce a complete module that can be technology transferred for characterizing the disease with minimal time and cost in the field conditions as well.

IV. CONCLUSION

By early control in charcoal rot, severe losses in soybean crop can be mitigated and hence crop yield can be enhanced significantly. Therefore, in this work, we developed a biospeckle based sensor for real-time characterization of charcoal rot in soybean crop. The results of this study indicated that the BA maps the progression of pathogen infection accurately for different time intervals and is highly responsive towards the disease symptoms even at early stage of infection. Furthermore, ability of the sensor to detect resistivity of different cultivars towards *M.phaseolina* was analyzed. Significant correlation between BA and data obtained from field trials showed that the proposed sensor has the potential to be used as a diagnostic tool for charcoal rot. Two new indexes (CSI and DSI) were proposed to estimate and quantify the intensity of infection and analyze susceptibility of each cultivar towards charcoal rot. The advantages of the proposed sensor as compared with the existing strategies include its high accuracy, extreme simplicity, automatic operation, high operating speed, minimal-cost, high performance efficiency, non-invasive identification, and user-friendliness. As part of the future work, we intend to develop a compact commercial product using laser biospeckle to characterize the effect of charcoal rot in soybean crop.

ACKNOWLEDGMENT

The authors are grateful to the anonymous reviewers for several constructive suggestions. These have resulted in

marked improvement of the content and presentation. They are also grateful to Dr. Subrato Guha, Professor of English, School of Comparative Languages and Culture, Devi Ahilya University, Indore, India for suggesting the syntactical corrections.

REFERENCES

- [1] M. C. Pagano and M. Miransari, "The importance of soybean production worldwide," in *Abiotic and Biotic Stresses in Soybean Production*, vol. 1, 1st ed. Oxford, U.K.: Elsevier, 2016, ch. 1, pp. 1–26.
- [2] M. Mohammad, "The importance of soybean production worldwide," in *Abiotic and Biotic Stresses in Soybean Production*, 1st ed. Oxford, U.K.: Academic, 2015, ch. 1, pp. 1–26.
- [3] G. L. Hartman, J. C. Rupe, E. J. Sikora, L. L. Domier, J. A. Davis, and K. L. Steffey, "Compendium of soybean diseases and pests," in *American Phytopathological Society*, 5th ed. Saint Paul, MI, USA: APS Press, 2015.
- [4] A. Wrather, G. Shannon, R. Balardin, L. Carregal, R. Escobar, G. K. Gupta, Z. Ma, W. Morel, D. Ploper, and A. Tenuta, "Effect of diseases on soybean yield in the top eight producing countries in 2006," *Plant Health Prog.*, vol. 11, no. 1, pp. 1–29, 2010.
- [5] V. Nataraj, S. Kumar, G. Kumawat, M. Shivakumar, L. S. Rajput, M. B. Ratnaparkhe, R. Ramteke, S. M. Gupta, G. K. Satpute, V. J. Rajesh, V. Kamble, and S. Chandra, "Charcoal rot resistance in soybean: Current understanding and future perspectives," in *Disease Resistance in Crop Plants*. Cham, Switzerland: Springer, 2019, pp. 241–259.
- [6] Vibha, P. Kumar, V. Gupta, A. Tiwari, and M. Kamle, Eds., "*Macrophomina phaseolina*: The most destructive soybean fungal pathogen of global concern," in *Current Trends in Plant Disease Diagnostics and Management Practices, Fungal Biology*, Springer, 2016, ch. 8, pp. 1–11.
- [7] A. F. Mahmoud, S. F. Abou-Elwafa, and T. Shehzad, "Identification of charcoal rot resistance QTLs in sorghum using association and in silico analyses," *J. Appl. Genet.*, vol. 59, no. 3, pp. 243–251, Aug. 2018.
- [8] A. Mengistu, J. D. Ray, J. R. Smith, and R. L. Paris, "Charcoal rot disease assessment of soybean genotypes using a colony-forming unit index," *Crop Sci.*, vol. 47, pp. 2453–2461, Aug. 2007.
- [9] M. Twizeyimana, C. Hill, M. Pawlowski, C. Paul, and G. L. Hartman, "A cut-stem inoculation technique to evaluate soybean for resistance to *macrophomina phaseolina*," *Plant Disease*, vol. 96, pp. 1210–1215, Aug. 2012.
- [10] C. H. Bock and F. W. Nutter, Jr., "Detection and measurement of plant disease symptoms using visible-wavelength photography and image analysis," *Plant Sci. Rev.*, vol. 6, p. 73, Aug. 2012.
- [11] M. Brouwer, B. Lievens, W. Van Hemelrijck, G. Van den Ackerveken, B. P. Cammue, and B. P. Thomma, "Quantification of disease progression of several microbial pathogens on *Arabidopsis thaliana* using real-time fluorescence PCR," *FEMS Microbiol. Lett.*, vol. 228, pp. 241–248, 2003.
- [12] A. H. Al-Ahmadi, A. Subedi, G. Wang, R. Choudhary, A. Fakhoury, and D. G. Watson, "Detection of charcoal rot (*Macrophomina phaseolina*) toxin effects in soybean (*Glycine max*) seedlings using hyperspectral spectroscopy," *Comput. Electron. Agric.*, vol. 150, pp. 188–195, Jul. 2018.
- [13] K. Nagasubramanian, S. Jones, S. Sarkar, A. K. Singh, A. Singh, and B. Ganapathysubramanian, "Hyperspectral band selection using genetic algorithm and support vector machines for early identification of charcoal rot disease in soybean stems," *Plant Methods*, vol. 14, p. 86, Dec. 2018.
- [14] A. Paul and N. Chaki, "Dimensionality reduction of hyperspectral images using pooling," *Pattern Recognit. Image Anal.*, vol. 29, no. 1, pp. 72–78, Jan. 2019.
- [15] W. E. Fry, "Introduction to disease management," in *Principles of Plant Disease Management*, 1st ed. New York, NY, USA: Academic, ch. 1, 2012, pp. 1–10.
- [16] J. Xia, B. Huang, Y. W. Yang, H. X. Cao, W. Zhang, L. Xu, Q. Wan, Y. Ke, W. Zhang, and D. Ge, "Hyperspectral identification and classification of oilseed rape waterlogging stress levels using parallel computing," *IEEE Access*, vol. 6, pp. 57663–57675, 2018.
- [17] W. Yang, C. Yang, Z. Hao, C. Xie, and M. Li, "Diagnosis of plant cold damage based on hyperspectral imaging and convolutional neural network," *IEEE Access*, vol. 7, pp. 118239–118248, 2019.
- [18] I. Potamitis and I. Rigakis, "Novel noise-robust optoacoustic sensors to identify insects through wingbeats," *IEEE Sensors J.*, vol. 15, no. 8, pp. 4621–4631, Apr. 2015.

- [19] J. Lee, S.-Y. Lee, R. E. Wijesinghe, N. K. Ravichandran, S. Han, P. Kim, M. Jeon, H.-Y. Jung, and J. Kim, "On-field *in situ* inspection for marssonina coronaria infected apple blotch based on non-invasive bio-photonics imaging module," *IEEE Access*, vol. 7, pp. 148684–148691, 2019.
- [20] J. W. Goodman, "Statistical properties of laser speckle patterns," *Laser Speckle and Related Phenomena*, 1st ed. Berlin, Germany: Springer, 1975, ch. 1, pp. 9–75.
- [21] A. Zdunek, A. Adamiak, P. M. Pieczywek, and A. Kurenda, "The biospeckle method for the investigation of agricultural crops: A review," *Opt. Lasers Eng.*, vol. 52, pp. 276–285, Jan. 2014.
- [22] P. Singh, A. Chatterjee, V. Bhatia, and S. Prakash, "Application of laser biospeckle analysis for assessment of seed priming treatments," *Comput. Electron. Agricult.*, vol. 169, pp. 1–13, Feb. 2020.
- [23] H. M. Van Der Kooij, R. Fokkink, J. Van Der Gucht, and J. Sprakel, "Quantitative imaging of heterogeneous dynamics in drying and aging paints," *Scientific Reports*, vol. 6, pp. 1–10, Sep. 2016.
- [24] A. Chatterjee, P. Singh, V. Bhatia, and S. Prakash, "Application of random temporal indexing based laser biospeckle analysis for blood thrombocyte characterization," in *Proc. Int. Conf. Fiber Opt. Photon. (PHOTONICS)*, New Delhi, India, Dec. 2018, pp. SP010-1–SP010-2.
- [25] P. Singh, A. Chatterjee, V. Bhatia, and S. Prakash, "A mobile phone based low cost biospeckle analysis tool for real time applications," in *Proc. Int. Conf. Fiber Opt. Photon. (PHOTONICS)*, New Delhi, India, Dec. 2018, pp. SP016-1–SP016-2.
- [26] A. Chatterjee, P. Singh, V. Bhatia, and S. Prakash, "A low-cost optical sensor for secured antispoof touchless palm print biometry," *IEEE Sensors Lett.*, vol. 2, no. 2, pp. 1–4, May 2018.
- [27] A. Chatterjee, V. Bhatia, and S. Prakash, "Anti-spoof touchless 3D fingerprint recognition system using single shot fringe projection and biospeckle analysis," *Opt. Lasers Eng.*, vol. 95, pp. 1–7, Aug. 2017.
- [28] A. Chatterjee, P. Singh, V. Bhatia, and S. Prakash, "Ear biometrics recognition using laser biospeckled fringe projection profilometry," *Opt. Laser Technol.*, vol. 112, pp. 368–378, Apr. 2019.
- [29] R. Dangi, P. Sinha, S. Islam, A. Gupta, A. Kumar, L. S. Rajput, D. Kamil, and A. Khar, "Screening of onion accessions for *Stemphylium* blight resistance under artificially inoculated field experiments," *Australas. Plant Pathol.*, vol. 48, pp. 375–384, Jul. 2019.
- [30] L. S. Rajput and S. I. Harlapur, "Cultural and morphological variability in *Rhizoctonia solani* causing banded leaf and sheath blight of maize," *Indian J. Plant Protection*, vol. 44, no. 1, pp. 165–167, 2016.
- [31] G. L. Cloud and J. C. Rupe, "Morphological instability on a chlo-rate medium of isolates of *Macrophomina phaseolina* from soybean and sorghum," *Phytopathology*, vol. 81, pp. 892–895, Aug. 1991.
- [32] A. Khambampati, D. Liu, S. Konki, and K. Kim, "An automatic detection of the ROI using Otsu thresholding in nonlinear difference EIT imaging," *IEEE Sensors J.*, vol. 18, no. 12, pp. 5133–5142, Apr. 2018.
- [33] R. A. Braga, R. J. González-Peña, D. C. Viana, and F. P. Rivera, "Dynamic laser speckle analyzed considering inhomogeneities in the biological sample," *J. Biomed. Opt.*, vol. 22, pp. 1–11, Apr. 2017.
- [34] M. H. Kutner, C. J. Nachtsheim, J. Neter, and W. Li, *Applied Linear Statistical Models*. 5th ed. New York, NY, USA: McGraw-Hill, 2005, ch. 3, pp. 100–153.
- [35] G. N. Agrios, "Parasitism and disease development," in *Plant Pathology*, 5th ed. Oxford, U.K.: Academic, 2005, ch. 2, pp. 79–103.
- [36] E. E. Ramírez-Miquet, J. G. Darias, I. Otero, D. Rodríguez, S. Murialdo, H. Rabal, and M. Trivi, "Biospeckle technique for monitoring bacterial colony growth with minimal photo-exposure time associated," in *VI Latin American Congress on Biomedical Engineering CLAIB*. Cham, Switzerland: Springer, 2015, pp. 313–316.
- [37] E. Simonetti, N. P. Viso, M. Montecchia, C. Zilli, K. Balestrasse, and M. Carmona, "Evaluation of native bacteria and manganese phosphite for alternative control of charcoal root rot of soybean," *Microbiol. Res.*, vol. 180, pp. 40–48, Nov. 2015.
- [38] A. Mengistu, J. R. Smith, J. D. Ray, and N. Bellaloui, "Seasonal progress of charcoal rot and its impact on soybean productivity," *Plant Disease*, vol. 95, no. 9, pp. 1159–1166, Sep. 2011.
- [39] L. M. Richards, S. S. Kazmi, J. L. Davis, K. E. Olin, and A. K. Dunn, "Low-cost laser speckle contrast imaging of blood flow using a Webcam," *Biomed. Opt. Exp.*, vol. 4, pp. 2269–2283, Oct. 2013.
- [40] A. Chatterjee, P. Singh, V. Bhatia, and S. Prakash, "An efficient automated biospeckle indexing strategy using morphological and geo-statistical descriptors," *Opt. Lasers Eng.*, vol. 134, pp. 17–31, Nov. 2020.



PUNEET SINGH (Graduate Student Member, IEEE) received the bachelor's degree in electronics and communication engineering from the Rajiv Gandhi Technical University, Bhopal, India, in 2013, and the M.E. degree in digital instrumentation from Devi Ahilya University, Indore, India, in 2017. He is currently pursuing the Ph.D. degree with the Electrical Engineering Department, Indian Institute of Technology Indore, India. His research interests are optical instrumentation,

biospeckle analysis, and smart agricultural solutions. He has published six journal publications and 14 conference proceedings, and has also filed two patents.



AMIT CHATTERJEE received the bachelor's degree in electronics and communication engineering from the Asansol Engineering College, West Bengal University of Technology, in 2014, and the master's degree in digital instrumentation from Devi Ahilya University, Indore, in 2016. He is currently pursuing the Ph.D. degree with the Electrical Engineering Department, Indian Institute of Technology-Indore, Indore, India. He currently has 26 publications and filed three patents.

His areas of interests include optical instrumentation, automated interferogram processing, and biospeckle analysis.



LAXMAN SINGH RAJPUT received the bachelor's degree in agriculture from ANGRAU, Hyderabad, in 2011, and the master's degree in agriculture from the College of Agriculture, UAS, Dharwad, India, in 2013. He has worked for management of banded leaf and sheath blight of maize and simulation model of cAMP dependent PKA in appressoria of *M. oryzae* under elevated temperature during his Ph.D. program. He is currently working as a Scientist (Plant Pathology) at the

Indian Institute of Soybean Research Institute, Indore. He has seven years of experience in management of plant disease and screening of genotypes against diseases. He also worked in effect on elevated temperature on rice blast resistance gene Pi 54. He has 12 peer-reviewed publications and one book chapter. He has received three gold medals during his M.Sc. (Agri) programme. During his Ph.D., he received the Senior Research Fellowship given by ICAR.



SANJEEV KUMAR received the bachelor's degree in agriculture from Agriculture College, Dapoli, Maharashtra, in 2012, and the master's degree in agriculture from the College of Agriculture, Hisar, India, in 2014. He is currently pursuing the Ph.D. degree in agriculture with ICAR- IARI, New Delhi, India. He has also worked as a Scientist (Plant Pathology) with the Indian Institute of Soybean Research, Indore. He has three years of experience in management of plant disease and screening of genotypes against diseases. He has worked on screening of tolerant callus against *Fusarium* wilt of chilli. He has seven peer-reviewed publications and one book chapter. Since 2017, he has been working on "Characterization of charcoal rot pathogen of soybean as well as involved in Soybean improvement against charcoal rot and anthracnose diseases."



VENNAMPALLY NATARAJ received the bachelor's degree in agriculture from ANGRAU, Hyderabad, in 2011, and the master's degree in agriculture from Banaras Hindu University (BHU), Varanasi, India, in 2013. He has seven years' experience in disease resistance breeding. He has worked on the research problem "Cytogenetic characterization and molecular mapping of *Triticum militinae* derived leaf rust resistance in wheat" during his Ph.D. program and identified and mapped a recessive gene derived from *Triticum militinae* governing wheat leaf rust resistance. This is world's first report on leaf rust resistance gene from *Triticum militinae*. Since 2017, he has been working on "Soybean improvement against charcoal rot and anthracnose diseases."



VIMAL BHATIA (Senior Member, IEEE) received the Ph.D. degree from the Institute for Digital Communications, The University of Edinburgh, Edinburgh, U.K., in 2005. He is currently working as a Professor with the Indian Institute of Technology Indore, India. He is also an adjunct faculty with IIT Delhi and IIIT Delhi, India. He has over 200 peer-reviewed publications, book chapters, and filed 11 patents. His research interests include the broader areas of non-Gaussian nonparametric signal processing with applications to communications. He is currently a Fellow of the IETE. During his Ph.D., he received the IEE fellowship for collaborative research on OFDM with Prof. Falconer with the Department of Systems and Computer Engineering, Carleton University, Ottawa, ON, Canada, and the Young Faculty Research Fellow from MeitY. He is also the General Co-Chair for IEEE ANTS 2018 and the General Vice-Chair for IEEE ANTS 2017. He is PI for external funding of over USD 2.0 million. He is a reviewer for the IEEE, OSA, Elsevier, Wiley, Springer, and IET.



SHASHI PRAKASH (Senior Member, IEEE) received the M.Tech. and Ph.D. degrees from the Indian Institute of Technology, Delhi, New Delhi, in 1992 and 2003, respectively. He joined Devi Ahilya University, Indore, India, as a Lecturer, in 1992, and was promoted to the post of Reader in 2002. From 1998 to 2000, he was a CSIR-Research Associate, working at the Indian Institute of Technology, Delhi. In 2009, he had a stint as 'Visiting Foreign Researcher' with the Department of Electrical and Electronics Engineering, Niigata University, Niigata, Japan. He is currently a Professor with the Department of Electronics and Instrumentation, Institute of Engineering and Technology, Devi Ahilya University. He has published more than 85 research papers in International conferences and journals. His research interests are in the area of optical metrology/communication.

...